


RESEARCH

Open Access



# Efficacy improvement of tri-serotypes vaccine for *Salmonella* using nanomaterial-based adjuvant in chicken

Hazem M. Ibrahim<sup>1</sup>, Gina M. Mohammed<sup>2</sup>, Rafik Hamed Sayed<sup>2</sup>, Hisham A. Elshoky<sup>3,4\*</sup> , Heba Elsayed Elzorkany<sup>3,4</sup> and Shaimaa Abdelall Elsaady<sup>2</sup>

## Abstract

**Background** This study aimed to develop a vaccine for controlling salmonellosis, a zoonotic disease affecting both humans and chicken, by employing Fe<sub>2</sub>O<sub>3</sub> ferrous iron oxide (FNPs), silicon dioxide (SiNPs), carboxymethyl chitosan (C.CS NPs), and FNPs-chitosan (FCNPs) nanocomposite as immunological adjuvants. The immune response of vaccinated chicken was assessed through ELISA and challenge tests.

**Results** The hydrodynamic diameters of Fe<sub>2</sub>O<sub>3</sub>, Fe<sub>2</sub>O<sub>3</sub>-CS, C.CS, and SiO<sub>2</sub> NPs were found to be 81.95 ± 14.95, 137.1 ± 20.5, 32.86 ± 14.05, and 15.64 ± 3.6 nm, respectively. The incorporation of nanoparticles into the vaccine formulation significantly enhanced its efficacy by eliciting a robust immune response. According to the study, FNPs, SiNPs, C.CS NPs, and FCNPs can be used as immunological adjuvants to strengthen chicken's immune systems and help prevent salmonellosis. By gradually raising antibody titers, all five vaccine formulations successfully stimulated an immunological response against *Salmonella* in vaccinated chicken. The size of the immunological response, however, differed amongst the various vaccination formulations. The SiNPs group had the highest antibody titer, followed by the locally administered vaccine.

**Conclusions** These findings suggest that the use of silicon dioxide SiNPs as a vaccine delivery system could enhance the immune response to *Salmonella* in chicken. Overall, the study demonstrates that the use of adjuvanted vaccines with nanomaterials, particularly SiNPs, has significantly increased the protection rate from 67 to 93.3% when compared to the locally used vaccine, which had a protection rate of 83%.

**Keywords** Adjuvant vaccine, Chitosan, Nanomaterials, *Salmonella*, Carboxymethyl chitosan, Silicon dioxide, Fe<sub>2</sub>O<sub>3</sub>

## 1 Background

Salmonellosis, which is an infectious disease transmitted between animals and humans, is caused by various strains of *Salmonella* bacteria. It poses a significant risk to public health and leads to substantial economic damage in the poultry industry and related products [1]. *Salmonella* infection poses a significant global public health challenge, with an estimated annual occurrence of 93.8 million cases and 155,000 deaths [2]. Poultry products serve as a major reservoir for *Salmonella* contamination, making it crucial to effectively manage *Salmonella* infection in poultry to reduce the risk of human transmission. Vaccination has proven to be a successful strategy in

\*Correspondence:

Hisham A. Elshoky  
heshamalshoky@sci.cu.edu.eg; heshamalshoky@gmail.com

<sup>1</sup> Department of Sera and Antigens Research, Veterinary Serum and Vaccine Research Institute, Agricultural Research Center, Cairo, Egypt

<sup>2</sup> Central Laboratory for Evaluation of Veterinary Biologics, Agricultural Research Center, Cairo, Egypt

<sup>3</sup> Nanotechnology and Advanced Materials Central Lab., Agricultural Research Center, Giza, Egypt

<sup>4</sup> Regional Center for Food and Feed, Agricultural Research Center, Giza, Egypt

controlling *Salmonella* infection in poultry. The potential contamination of chicken eggs by specific serotypes like *Salmonella enterica* and *Salmonella typhimurium* raises notable concerns [3]. To control the spread of salmonellosis, vaccination is a key strategy, especially in chicken, to prevent the spread of infection to humans [4].

Numerous authors have documented the development of inactivated vaccines to prevent and manage avian salmonellosis. Additionally, a trivalent *Salmonella* vaccine, produced locally, is currently accessible in the Egyptian market [5, 6]. These vaccines primarily aim to protect poultry from different serovars of *Salmonella*, including *Salmonella enteritidis* and *Salmonella typhimurium*, which are known to cause significant health issues in poultry populations. The existing vaccines typically consist of inactivated or attenuated strains of *Salmonella* that are administered to poultry to stimulate an immune response. However, despite the availability of these vaccines, there is a pressing need for improved *Salmonella* vaccines in the poultry industry. The current vaccines, while effective to a certain extent, may not provide comprehensive protection against all prevalent serovars or strains of *Salmonella*. Moreover, evolving strains of *Salmonella* with altered antigenic profiles may reduce the efficacy of existing vaccines [7–10]. Nowadays, our life is so fast as well as ways of manufacturing vaccines. Nanotechnology has revolutionized vaccine manufacturing, with the use of nanomaterials as adjuvants being of particular interest, by harnessing the unique properties of nanomaterials. Their small size and strong affinity for microorganisms make them highly effective adjuvants in vaccines [11]. Recently, nanoparticles had several clinical uses for diagnostic and therapeutic purposes, e.g., drug carrier [12] and vaccine adjuvant [13, 14]. One of the significant advantages of using nanomaterials for vaccine development is their ability to enhance the immune response. Conventional vaccines often elicit weak or short-lived immune responses, particularly in the case of infectious diseases that are challenging-to-control infectious diseases, such as bovine tuberculosis, brucellosis, and foot-and-mouth disease. Nanoparticles can act as adjuvants, boosting immune responses in vaccines by stimulating both the innate and adaptive immune systems for a stronger and long-lasting immune response [15]. Furthermore, nanoparticles can be tailored to target specific cells or tissues, rendering them more efficient in vaccine delivery [16].

Metal oxide nanoparticles as iron and silicon dioxide nanoparticles offer distinct advantages compared to other nanoparticles. Iron nanoparticles have gained significant attention as vaccine adjuvants, displaying promising results in various studies. Their robust structure ensures stability for biomedical applications and makes

them ideal for designing novel carriers and vaccine adjuvants [17]. Similarly, silicon dioxide ( $\text{SiO}_2$ ) has emerged as a promising adjuvant for the development of innovative preventive and therapeutic vaccines [18].  $\text{SiO}_2$  is a widely studied nanomaterial that enhances immune responses by facilitating antigen uptake and presentation, activating dendritic cells, and promoting proinflammatory cytokines production [19, 20].

In contrast, polymeric nanoparticles like chitosan nanoparticles are widely used in vaccine manufacturing as adjuvants added to vaccines to boost immunity because of their biocompatibility, biodegradability, and enhanced bioavailability [21–23]. Carboxymethyl chitosan nanomaterials (C.CS) is a water-soluble derivative of chitosan, a natural biopolymer that is a derivative of chitin. C.CS was evaluated as an adjuvant in a live attenuated *Salmonella* vaccine in chicken [24]. The results showed that the inclusion of C.CS resulted in elevated antibody production, enhanced lymphocyte proliferation, and a strengthened immune response in comparison with the vaccine lacking C.CS. The researchers concluded that C.CS could be used as an effective adjuvant in poultry vaccines against *Salmonella* infection [24].

It was worth studying that the efficiency of iron oxide nanoparticles (FNPs), silicon dioxide nanoparticles (SiNPs), carboxymethyl chitosan nanoparticles (C.CS NPs), and iron oxide with chitosan nanoparticles (FCNPs) was deemed important due to their favorable attributes including safety profiles, water solubility, applicability as drug delivery systems, and cost-effective production, chitosan nanoparticles have emerged as a novel adjuvant for managing salmonellosis disease. The objective of this study is to develop and assess innovative vaccines to control salmonellosis disease by using  $\text{Fe}_2\text{O}_3$  NPs,  $\text{Fe}_2\text{O}_3$ -CS NPs, C.CS NPs, and  $\text{SiO}_2$  NPs as immunological adjuvant boosting the immune system of chicken comparing with locally produced *Salmonella* vaccine. This study endeavors to shed light on the necessity for enhanced *Salmonella* vaccines, identifying areas of improvement and contributing to the ultimate objective of developing superior adjuvant vaccines.

## 2 Methods

### 2.1 Bacterial strains

The strains of bacteria employed in this research were obtained from chicken sources and generously supplied by the Bacterial Sera and Antigens Research Department at the Veterinary Serum and Vaccine Research Institute (VSVRI) in Abbasia, Cairo, Egypt. The *Salmonella* strains selected for this research were *S. Typhimurium*, *S. Kentucky*, and *S. Enteritidis*, which were identified as distinct types of *Salmonella* using morphological and biochemical identification techniques, including the VITEK 2®

COMPACT procedure developed by Biomerieux. A bacterial vaccine was produced by culturing a mixture of the three *Salmonella* bacterial cells (referred to as 3S-bacteria) in Luria broth (LB) medium, with a final concentration of  $1 \times 10^{10}$  colony-forming units per milliliter (CFU/mL), and the mixture was incubated at 37 °C for 24 h.

## 2.2 Preparation of vaccinal strains

From the Bacterial Sera and Antigens Research Department, VSVRI, three isolated *Salmonella* strains (*S. Typhimurium*, *S. Kentucky*, and *S. Enteritidis*) isolated from chicken were obtained and employed in the creation of vaccines. Separate strains of *S. Typhimurium*, *S. Kentucky*, and *S. Enteritidis* were cultured for 24 h at 37 °C on S.S. agar. Selected colonies of each type were inoculated separately on broth of tryptone soya and incubated for 24 h at 37 °C. The total colony count technique was used to modify the bacterial suspension to have  $1 \times 10^{10}$  CFU/mL. Using the total colony count method, the final suspension of each bacterium was adjusted to contain  $2 \times 10^{10}$  CFU/mL [25]. The commercially available locally inactivated trivalent *Salmonella* vaccine, serving as the positive control, was generously provided by the Sera and Antigens Research Department at VSVRI.

## 2.3 Preparation of nanomaterials

Synthesis, preparation, and characterization of nanomaterials have been carried out at Nanotechnology and Advanced Materials Central Lab., Agricultural Research Center. The  $\text{Fe}_2\text{O}_3$  nanoparticles (FNPs) were prepared according to [26] with modification. Briefly, in a three-necked flask 12 g of ferric chloride anhydrous was added to 150 mL oleylamine with stirring under argon gas. Afterward, the solution underwent reflux at a temperature of 110 °C for 1 h, and then, the mixture was transferred to the oven at 300 °C for 2 h. The precipitant was washed thrice times, a mixture of water/ethanol, and collected by centrifugation. Subsequently, the iron oxide was dried in an oven for 8 h at 120 °C, followed by fine grinding and storage. To attain a concentration of 1 mg/mL, the prepared iron oxide nanoparticles (FNPs) were added to 10 mL of deionized  $\text{H}_2\text{O}$  containing 50  $\mu\text{L}$  of Tween 80. The solution was then subjected to ultrasound waves using the Hielscher UP400St ultrasonicator (25 W, A 45%, contentious) for 10 min while being placed in an ice bath until it became well-suspended.

Carboxymethyl chitosan (C.CS) was prepared according to [27] with modification, and 20 g of NaOH was dissolved in 200 mL warm deionized  $\text{H}_2\text{O}$ , then 5 gm chitosan low M.wt (Acros organics) was added, and after overnight stirring 50 mL of 1 g/mL monochloroacetic acid (Sigma, USA) was added dropwise, after the complete addition the solution was kept under stirring at 40

°C for 2 h, at the end the pH was adjusted to pH 7.4 to neutralize the solution. Then, 300 mL of 70% methanol was added, and the solution was kept stirred overnight. Thereafter, the solution was centrifuged at 4700 rpm, 10 °C, 15 min. Then, it was washed thrice and kept in a vacuum oven overnight at 60 °C. Following this process, a pale-yellow powder was obtained. Then, a solution of 100 mg of C.CS was dissolved in 20 mL of deionized water containing 1 mL of glacial acetic acid and left to stir overnight. Subsequently, 8 mg of sodium tripolyphosphate (TPP) was added dropwise to the C.CS solution in 5 mL of water, and the mixture was stirred for 30 min. After that, we obtain C.CS nanoparticles.

According to a previous report by [28], a composite of  $\text{Fe}_2\text{O}_3$ -chitosan nanoparticles (FCNPs) was prepared with a modification that  $\text{Fe}_2\text{O}_3$  was used instead of  $\text{Fe}_3\text{O}_4$ . To prepare the FCNPs, 100 mg of chitosan was dissolved in a solution containing 2 mL of glacial acetic acid and 100 mL of distilled water. The solution was homogenized at room temperature for 3 h using a homogenizer at 10,000 rpm. Afterward, homogenization was carried on after additions of 100 mg of polyvinylpyrrolidone (PVP) for another 3 h. 38 mg of  $\text{Fe}_2\text{O}_3$  nanoparticles was then added, and the homogenization was continued overnight. A final homogenization step was carried out for 30 min after the addition of 33 mg of TPP at a concentration of 5 mg/mL.

Silicon dioxide nanoparticles (SiNPs) were synthesized by sol-gel process [29]. Briefly, 45 mL of tetraethylorthosilicate (TEOS 98%, Sigma-Aldrich, USA) was added to 600 mL 50% ethanol and sonicated for 10 min followed by the addition of 15 mL ammonium hydroxide ( $\text{NH}_4\text{OH}$ , 33%) and then stirred overnight at room temperature; finally, the prepared SiNPs were dispersed in 20 mL 50% ethanol to achieve a final concentration of 1 mg/mL. The solution suspension was achieved by placing it on ice and exposing it to ultrasound waves for 30 min using the Hielscher UP400St ultrasonicator (25 W, A 45%, contentious).

## 2.4 Minimal inhibition concentration (MIC) of nanoparticles

MIC of various concentrations of the four prepared nanoparticles was estimated as follows: in different tubes 200, 400, 600, and 800  $\mu\text{g}/\text{mL}$  of each nanomaterial was added to 5 mL Luria broth (LB) culture medium containing  $10^{10}$  CFU/mL of the Tri *Salmonella* strains and incubated for 24 h at 37 °C [30]. 50  $\mu\text{L}$  of the bacterial suspension was then spread onto S.S agar and incubated for a further 24 h, and then, the CFU count growing on agar was noted, and the survival of treated bacteria is calculated according to Eq. 1:

$$\text{Survival percentage relative to control (\%)} = \frac{\text{CFU NPs}}{\text{CFU Control}} \quad (1)$$

## 2.5 Estimation of live/dead bacteria by confocal microscopy

To evaluate whether the bacteria were viable, the Tri *Salmonella* strains were exposed to varying concentrations of the four nanomaterials separately. The viability of the treated bacteria was determined by utilizing confocal fluorescence microscopy (LSM 710, Carl Zeiss, Germany). The live/dead ratio of the bacterial cells was determined by incubating 100  $\mu\text{L}$  of 3S-bacteria with a 1:1 mixture of propidium iodide (PI) and acridine orange (AO) stains and then examining the cells using an EC Plan-Neofluar 40x/1.3 oil objective after 15 min of incubation in the dark. While acridine orange (AO) was utilized to stain the live cells and displayed green fluorescence, propidium iodide (PI) could only penetrate the membranes of dead cells and displayed red fluorescence. The viable cell ratios in both the control and treated samples were determined using Zen Blue 3.3 software. The viability of the cells is calculated using Eq. 2.

$$\text{Live bacteria\%} = \frac{\text{intensity of (AO) in treated sample} * 100}{\text{intensity of (AO) in control}} \quad (2)$$

## 2.6 Physicochemical characterization of nanoparticles

To examine the properties of the synthesized nanomaterials, various characterization techniques were employed. The dynamic light scattering technique was utilized to assess the average size distribution of the nanoparticles. Zeta potentials (ZPs) were measured using the Zetasizer Nano Series (Malvern, ZS Nano, UK). Transmission electron microscopy (TEM; Thermo Scientific Talos F200i, Thermo Fisher, Netherlands) operating at 200 kV was employed for morphological characterization. The nanomaterials were dried overnight at 80 °C in a vacuum oven. X-ray diffraction (XRD) patterns were obtained using an X'Pert-Pro X-ray diffractometer (Panalytical, Netherlands) with Cu-K radiation, covering a range of 10°–70°.

## 2.7 SERVAC inactivated Tri. Sal. Vaccine

This vaccine was supplied by the Bacterial Sera and Antigens Research Department at the Veterinary Serum and Vaccine Research Institute (VSVRI) in Abbasia, Cairo, Egypt. It contains three *Salmonella* strains (*S. Typhimurium*, *S. Kentucky*, and *S. Enteritidis*), Batch No. 2104 Expiry date 10/2023. It was used for the vaccination of the control group in the experimental design. The adjuvant-enhanced vaccine was formulated through the incorporation of  $1 \times 10^{10}$  trivalent *Salmonella* with 400

$\mu\text{L/ml}$  nanoparticles for each nanocomposite. The mixture was then vigorously shaken for one hour before being refrigerated for storage until needed.

## 2.8 Chicken

A total of 280 specific pathogen-free (SPF) broiler chicken, aged 2 weeks and vaccinated against Newcastle, Mycoplasma, and Marek's diseases, were sourced from the SPF farm Kom-Oshim, Fayoum, Egypt. These chicken were housed in isolators at the animal husbandry facilities of the Central Laboratory for Evaluation of Veterinary Biologics, Cairo, Egypt. Prior to the study, the chicken were tested using ELISA to confirm their freedom from *Salmonella* infection and antibodies. Throughout the study, the chicken were provided with unrestricted access to feed that did not contain any antibacterial or anticoccidial components.

## 2.9 Experimental design

A total of 180 SPF 2 weeks old for chicken were assigned to six groups for the study. Each group received first dose (0.5 ml/os (Oral Administration route) of vaccine at 3 weeks of age; then, a booster dose was administered after three weeks at five weeks of age. The vaccines were stored in a refrigerator, and for the experimental trial, transportation was done using an ice box. Group 1 (FNPs-G<sub>1</sub>) received a Tri-*Salmonella* vaccine with ferric oxide adjuvant via oral route ( $1 \times 10^{10}$  CFU/dose) and included 30 chickens. Group 2 (FCNPs-G<sub>2</sub>) also received the Tri-*Salmonella* vaccine with ferric oxide adjuvant and chitosan. Group 3 (C.CS-G<sub>3</sub>) received the Tri-*Salmonella* vaccine with carboxy methyl chitosan adjuvant. Group 4 (SiNPs-G<sub>4</sub>) received the Tri-*Salmonella* vaccine with silicon dioxide adjuvant. Group 5 (V-G<sub>5</sub>) received an inactivated Trivalent *Salmonella* vaccine adjuvanted by formalin. Group G<sub>6</sub>, consisting of 30 chicken, was injected with 0.5 mL/os of normal saline and served as the control group. Blood samples were collected before vaccination, three weeks after vaccination (once per week), and three weeks after boosting (once per week). The samples were pooled and stored at -20 °C for further investigation of the antibodies induced by the vaccination.

## 2.10 Prepared vaccine quality control

### 2.10.1 Sterility test

The prepared vaccine underwent rigorous testing to confirm its freedom from contamination, including aerobic and anaerobic bacteria as well as fungi. This was done by inoculating the vaccine on thioglycolate broth and

incubated for 48–72 h at 37 °C and on soya casein digestive agar at 25 °C for 14 days [31].

### 2.10.2 Safety test

A total of 100 specific pathogen-free (SPF) chickens, aged 2 weeks, were utilized for the safety evaluation of the prepared vaccines [31]. The safety test involved administering a double field dose (1 mL) of each vaccine orally to 20 SPF chickens aged 2 weeks for each vaccine. These chickens were closely monitored for two weeks to detect any local reactions, clinical signs, or mortality [31].

### 2.10.3 Immune response analysis of the prepared vaccines

**2.10.3.1 Enzyme-Linked Immunosorbent Assay (ELISA)** The elimination of bacteria from the immune system is crucial for a protective response against *Salmonella*, and antibodies play a key role in this process. The humoral immune response against *Salmonella* antigens in the prepared vaccine was evaluated using an ELISA assay with a *Salmonella* antibody test kit (BioChek poultry immunoassays cat # CK117 for *S. enteritidis* and CK118 for *S. typhimurium*) according to the kit manufacturer's manual. Serum from SPF chicken diluted in phosphate buffer with protein stabilizer and sodium azide as a preservative (0.1% w/v) was used as a negative control. Antiserum containing antibodies specific to *S. enteritidis* in phosphate buffer with protein stabilizers and sodium azide preservative (0.1% W/V) was used as a positive control.

**2.10.3.2 Reagent preparation** The microtiter plates coated with either *S. enteritidis* or *S. typhimurium* LPS were charged with 100 µL of diluted serum samples 1:500. Positive and negative controls were included. The plates were incubated at room temperature (22–27 °C) for 30 min. Subsequently, the well contents were aspirated and washed 4 times with wash buffer (300µL per well). Next, 100 µL of the conjugate reagent was added to the appropriate wells and incubated as before, followed by 5 washes with washing buffer. Afterward, 100 µL of the substrate reagent was added to the appropriate wells and incubated at room temperature for 15 min. Finally, 100 µL of stopping solution was added, and the absorbance was measured at 405 nm using a microtiter plate reader. The S/P ratio is calculated using Eq. 3.

$$S/P = \frac{\text{mean of test sample} - \text{mean of negative control}}{\text{mean of positive control} - \text{mean of negative control}} \quad (3)$$

While the antibody titer is counted as Eq. 4:

$$\text{Log}_{10} \text{Titre} = 1.13 \text{ Log} (S/P) + 3.156 \quad (4)$$

$$\text{AntiLog} = \text{Antibody titer}$$

where S is the test sample, P is positive control.

**2.10.3.3 Evaluation of humoral immune response against *Salmonella* Kentucky in the vaccinated chicken** The antibody response generated against *Salmonella* Kentucky in the vaccinated chicken was assessed in the serum using a homemade ELISA method based on Haider A. Mousa's protocol from 2007 [32]. The calculation of the antibody titers was similar to that of *S. enteritidis* and *S. typhimurium*.

### 2.10.4 Challenge test

Each group was further divided into three subgroups, and four weeks after the booster dose, each subgroup was orally challenged with 1mL of a solution containing  $1 \times 10^8$  CFU of each strain (*S. Kentucky*, *S. Typhimurium*, and *S. Enteritidis*) separately [21]. The chicken that received the challenge were observed for a month, and the protection rate was determined based on the severity of clinical signs, mortality, and recovery of the challenge organisms from fecal samples. Fecal samples were collected before the start of the experiment and weekly for four weeks after the challenge using sterile swabs. These samples, collected from both vaccinated and control chickens, were inoculated into tetrathionate broth and examined bacteriologically for the presence of *Salmonella* shedding, following the method described by Cruickshank et al. in 1987 [33].

$$\text{Protection \%} = \left( \frac{\text{Survived chicken}}{\text{total number of chicken}} \right) \times 100$$

### 2.11 Statistical analysis

The statistical analysis was done using GraphPad prism software version 8.0.2. ELISA results were analyzed and compared with parametrical correlation using the one-way ANOVA and two-way ANOVA test [34]. \* Significant at  $p < 0.05$ , \*\* significant at  $p < 0.01$ , \*\*\* significant at  $p < 0.001$ , and \*\*\*\* significant at  $p < 0.0001$ .

### 2.12 Ethical approval

The research manuscript has been reviewed and acknowledged by the Institutional Animal Care and Use Committee at the Central Laboratory for Evaluation of Veterinary Biologics. It has been determined that the manuscript is in compliance with bioethical standards and has been approved for research purposes.

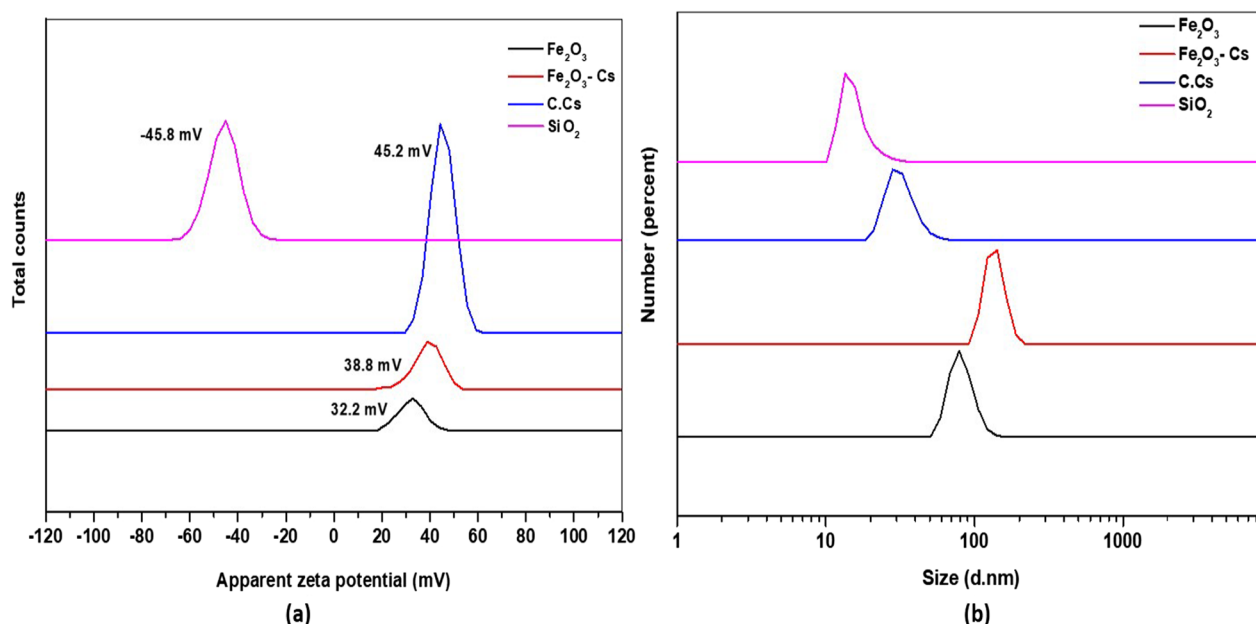


**Fig. 1** **a** The zeta potential measurements of Fe<sub>2</sub>O<sub>3</sub>, Fe<sub>2</sub>O<sub>3</sub>-CS, C.CS, and SiO<sub>2</sub> nanomaterials. **b** The distribution of the hydrodynamic diameter in nm of Fe<sub>2</sub>O<sub>3</sub>, Fe<sub>2</sub>O<sub>3</sub>-CS, C.CS, and SiO<sub>2</sub> nanomaterials

### 3 Results

#### 3.1 Characterization of nanomaterials

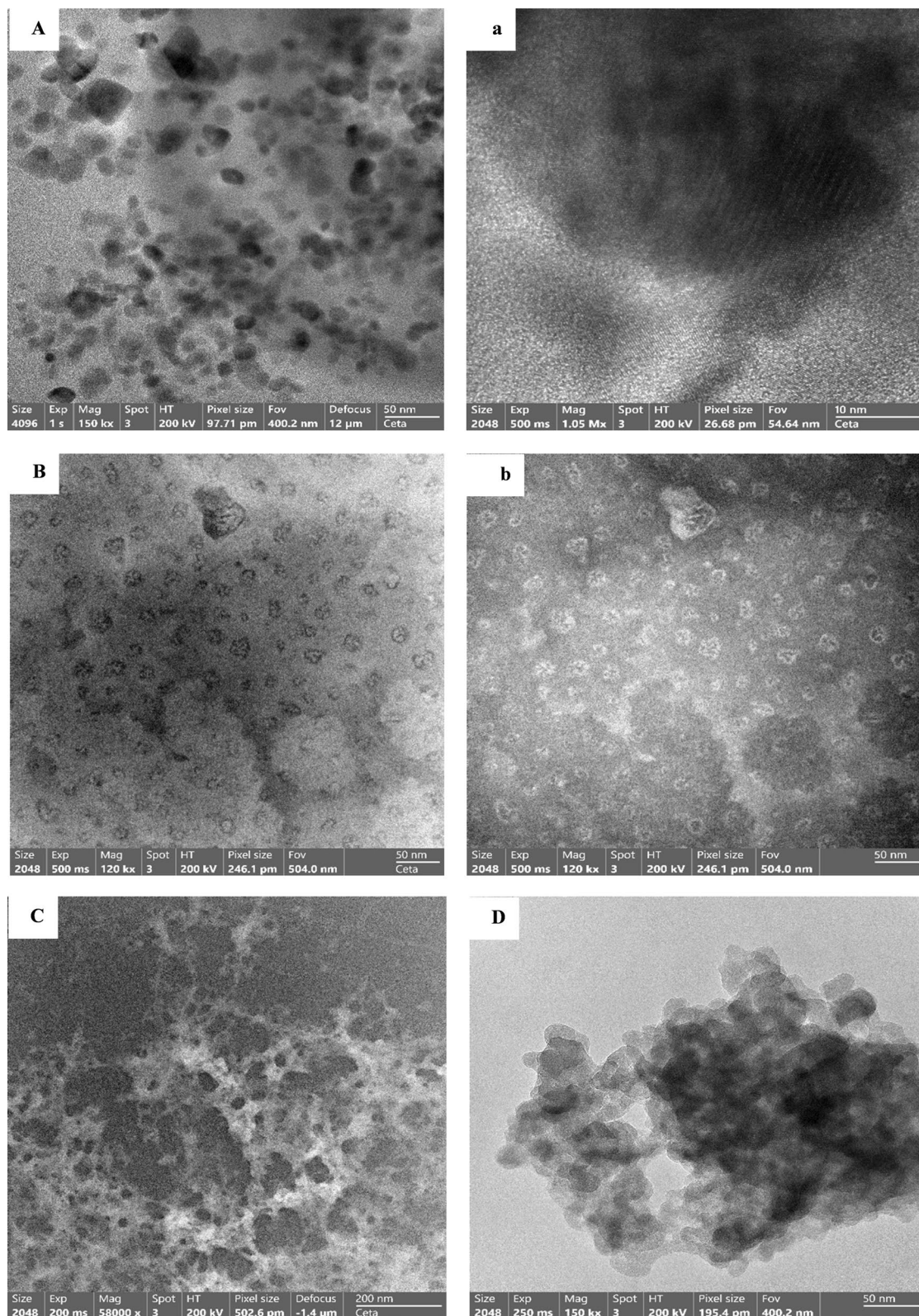
The zeta potential measurements of the Fe<sub>2</sub>O<sub>3</sub> NPs, Fe<sub>2</sub>O<sub>3</sub>-CS NPs, C.CS NPs, and SiO<sub>2</sub> NPs are presented in Fig. 1a. This figure shows that the Fe<sub>2</sub>O<sub>3</sub> and Fe<sub>2</sub>O<sub>3</sub>-CS NPs have a zeta potential of  $32.2 \pm 5.01$ , and  $38.8 \pm 6.06$  mV. Furthermore, the zeta potential of C.CS and SiO<sub>2</sub> NPs is equal to  $45.2 \pm 5.02$  and  $-45.8 \pm 6.14$  mV, respectively. All nanoparticles that have been prepared exhibit a zeta potential surpassing the range of  $\pm 30$  mV, which serves as a clear indication of the particles' robust stability within the solution [28, 35–37].

Figure 1b presents the distribution of the hydrodynamic diameter of the prepared nanomaterials, including Fe<sub>2</sub>O<sub>3</sub>, Fe<sub>2</sub>O<sub>3</sub>-CS, C.CS, and SiO<sub>2</sub> nanomaterials as measured using dynamic light scattering (DLS). The Fe<sub>2</sub>O<sub>3</sub>, Fe<sub>2</sub>O<sub>3</sub>-CS NPs, C.CS NPs, and SiO<sub>2</sub> NPs had hydrodynamic diameters of  $81.95 \pm 14.95$ ,  $137.1 \pm 20.5$ ,  $32.86 \pm 14.05$ , and  $15.64 \pm 3.6$  nm, respectively.

TEM was employed to examine and present the uniformity and dimensions of the Fe<sub>2</sub>O<sub>3</sub> nanoparticles (NPs), Fe<sub>2</sub>O<sub>3</sub>-CS NPs, C.CS NPs, and SiO<sub>2</sub> NPs, as illustrated in Fig. 2A–D. The size of the crystalline structures was determined using Scherrer analysis based on the diffraction pattern's peak broadening caused by finite-sized crystals. The estimated crystalline size was approximately 19 nm, which closely matched the particle sizes observed via TEM, indicating a high level of crystallinity in the synthesized hematite nanoparticles. Figure 2A displays

monodisperse, spherical hematite nanoparticles with a diameter of approximately 20 nm, exhibiting a mica-ceous nature (extremely thin layers). Figure 2B depicts TEM images of the Fe<sub>2</sub>O<sub>3</sub>-CS NPs, showcasing two distinct morphologies: spherical particles with a diameter of about 21–40 nm and CS forms a layer of small particles coating on the surface of Fe<sub>2</sub>O<sub>3</sub> NPs. This is easily observed when utilizing inverse gray scaling. In this representation, iron is depicted as white, and CS is depicted as clustered black spots on the iron surface. In a regular window, chitosan is seen as white clusters indicating successful iron oxide doping of the chitosan nanoparticles. Figure 2C presents the TEM image of C.CS NPs, demonstrating a nearly uniform structure. Finally, Fig. 2D displays the TEM image of SiO<sub>2</sub> NPs, revealing well-formed, semi-spherical structures with an average diameter of approximately 30 nm.

Figure 3 presents that the X-ray diffraction (XRD) pattern of the synthesized nanoparticles is depicted in the figure. Analyzing the XRD pattern of SiO<sub>2</sub> NPs confirms their amorphous nature, as indicated by the characteristic diffraction broad peak centered at  $23^\circ$  ( $2\theta$ ). Furthermore, the XRD pattern of C.CS reveals a semi-crystalline structure, evident from the distinctive peak observed around  $19^\circ$ . This figure also presents the XRD patterns of Fe<sub>2</sub>O<sub>3</sub> and Fe<sub>2</sub>O<sub>3</sub>-CS NPs. The X-ray diffraction (XRD) analysis revealed distinct peaks in the Fe<sub>2</sub>O<sub>3</sub> sample at  $2\theta$  values of  $30.06^\circ$ ,  $33.18^\circ$ ,  $35.62^\circ$ ,  $43.14^\circ$ ,  $47.62^\circ$ ,  $53.74^\circ$ ,  $57.18^\circ$ , and  $62.14^\circ$  corresponding to the crystallographic



**Fig. 2** TEM images of  $\text{Fe}_2\text{O}_3$ ,  $\text{Fe}_2\text{O}_3\text{-CS}$ ,  $\text{C.CS}$ , and  $\text{SiO}_2$  nanomaterials, respectively

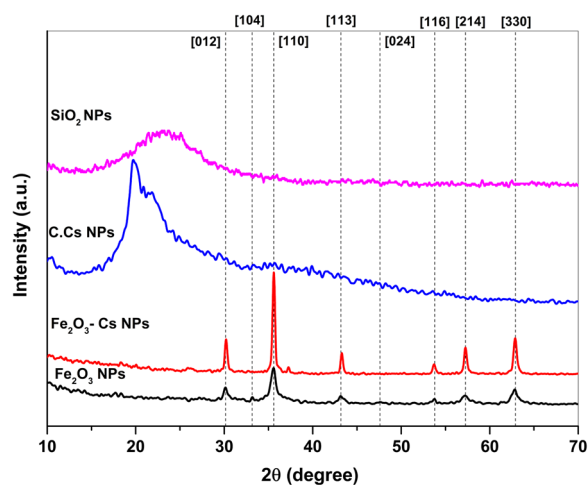


**Fig. 3** X-ray diffraction patterns of  $\text{Fe}_2\text{O}_3$ ,  $\text{Fe}_2\text{O}_3$ -CS, C.CS, and  $\text{SiO}_2$  nanomaterials, respectively

planes (012), (104), (110), (113), (024), (116), (214), and (330), respectively. These findings closely match the standard XRD pattern (JCPDS File No. 01-073-3825) for hematite, confirming the presence of hematite in the synthesized nanoparticles. Furthermore, the XRD pattern of  $\text{Fe}_2\text{O}_3$ -CS NPs demonstrated that the coating process did not induce any phase changes in the iron oxide. Additionally, a weak diffraction peak of CS was observed at approximately  $20^\circ$  (JCPDS File No. 04-008-8146). However, in the XRD pattern of  $\text{Fe}_2\text{O}_3$ -CS NPs, the intensity of the CS peak was significantly reduced and shifted to  $25^\circ$  due to its binding to  $\text{Fe}_2\text{O}_3$  NPs through the interaction of the OH group.

### 3.2 Quality control of prepared vaccines

The prepared vaccines for immunization of chicken were proved to be safe and free of bacterial and fungal contamination (Fig. 4).

### 3.3 The minimal inhibition concentration of nanoparticles

Table 1 shows that the MIC of  $\text{Fe}_2\text{O}_3$  NPs was 10 mg/mL with 85%, while the MIC of  $\text{Fe}_2\text{O}_3$ -CS NPs was 600  $\mu\text{g}/\text{mL}$  with 93%, the MIC of C.CS NPs was 600  $\mu\text{g}/\text{mL}$  with 95%; furthermore, the MIC of  $\text{SiO}_2$  NPs was 600  $\mu\text{g}/\text{mL}$  with 97% for inhibition growth of three *Salmonella* strains. Serial dilutions of 200, 400, 600, and 800  $\mu\text{g}/\text{mL}$  were prepared, and the MIC of the synthesized  $\text{Fe}_2\text{O}_3$  NPs was found to be 550  $\mu\text{g}/\text{mL}$ .

## 4 Confocal live/dead imaging

In our study, we aimed to investigate the effect of different nanomaterials on the viability of live/dead 3S-bacteria. To achieve this, we incubated the bacteria with

varying concentrations of four different nanomaterials and assessed their viability using confocal microscopy imaging. We stained viable cells with AO, which emits a green signal, and dead cells with PI, which emits a red signal. This allowed us to clearly distinguish between live and dead bacteria under the microscope. To quantify the effects of the nanomaterials, we used Zen software to calculate the ratios of viable cells in both control and treated samples based on AO emission intensity. Our results showed that at a concentration of 200  $\mu\text{g}/\text{mL}$ , all four types of nanomaterials had no significant effect on bacterial viability, as indicated by the similar ratios of viable cells in control and treated samples. However, when we increased the concentration to 400  $\mu\text{g}/\text{mL}$ , only SiNPs did not show significant reduction in bacterial viability, whereas all other types of nanomaterials exhibited high antibacterial activity.

### 4.1 Evaluation of the immune response of the prepared nanovaccines

#### 4.1.1 ELISA test

Antibodies play a crucial role in demonstrating the immune response of vaccinated chickens against *Salmonella*. The immune response of vaccinated chickens against *S. Typhimurium*, as depicted in Fig. 5. A, revealed the antibody titers for different groups. In the FNPs-G1 group, the antibody titer was 327 in the first week post-vaccination, which increased to 568 in the third week post-vaccination. After booster immunization, the antibody titer further rose from 597 in the first week post-boostering to 861 in the third week post-boostering. For the FCNPs-G2 group, the antibody titer was 332 in the first week post-vaccination, reaching 582 in the third week post-vaccination.

Following booster immunization, the antibody titer increased from 685 in the first week post-boostering to 810 in the third week post-boostering. In the C.CS-G3 group, the antibody titer was 280 in the first week post-vaccination, which rose to 481 in the third week post-vaccination. After booster immunization, the antibody titer increased from 531 in the first week post-boostering to 654 in the third week post-boostering. The SiNPs-G4 group displayed an antibody titer of 558 in the first week post-vaccination, which increased to 842 in the third week post-vaccination. The antibody titer rose significantly from 1145 in the first week post-boostering to 2001 in the third week post-boostering. In the V-G5 group, the antibody titer was 184 in the first week post-vaccination, reaching 900 in the third week post-vaccination. After booster immunization, the antibody titer increased from 905 in the first week post-boostering to 1225 in the third week post-boostering. Statistical analysis revealed a



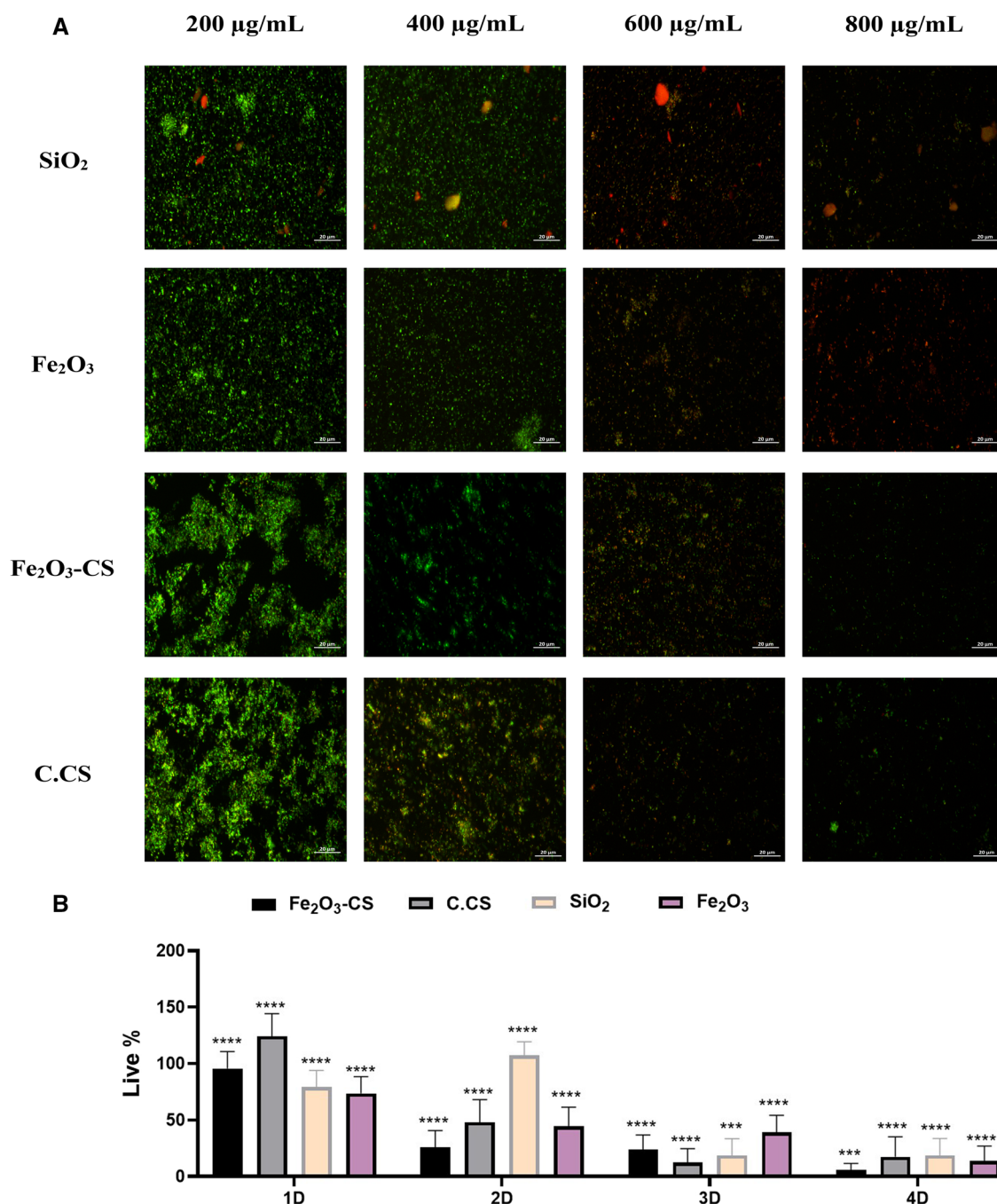


**Fig. 4** **a** Confocal images of live/dead 3S-bacteria stained with AO/PI, respectively, scale bar 20 µm. **b** Live/dead ratio relative to control calculated from fluorescence intensity that analyzed by Zen software. Significant at  $p < 0.05$ ,  $**p < 0.01$ ,  $***p < 0.001$ , and  $****p < 0.0001$

significant difference among the groups, with the SiNPs-G4 group exhibiting the highest antibody titer compared to the other groups.

In Fig. 5B, depicting the immune response against *S. Kentucky*, variations in antibody titers were observed across groups. For instance, the SiNPs-G4 group exhibited a substantial rise in antibody titer from 538 (first

week post-vaccination) to 1938 (third week post-booster) after booster immunization. Contrastingly, the V-G5 group showed a more modest increase in titer from 200 (first week post-vaccination) to 1100 (third week post-booster).

Figure 5C portrays the immune response against *S. Enteritidis*. The FNPs-G1 group displayed an antibody

**Table 1** MIC of different nanomaterials

	200 µg/mL	400 µg/mL	600 µg/mL	800 µg/mL
Fe <sub>2</sub> O <sub>3</sub>	40%	65%	85%	0%
Fe <sub>2</sub> O <sub>3</sub> +CS	50%	75%	93%	0%
C.CS	45%	70%	95%	0%
SiO <sub>2</sub>	55%	80%	97%	0%

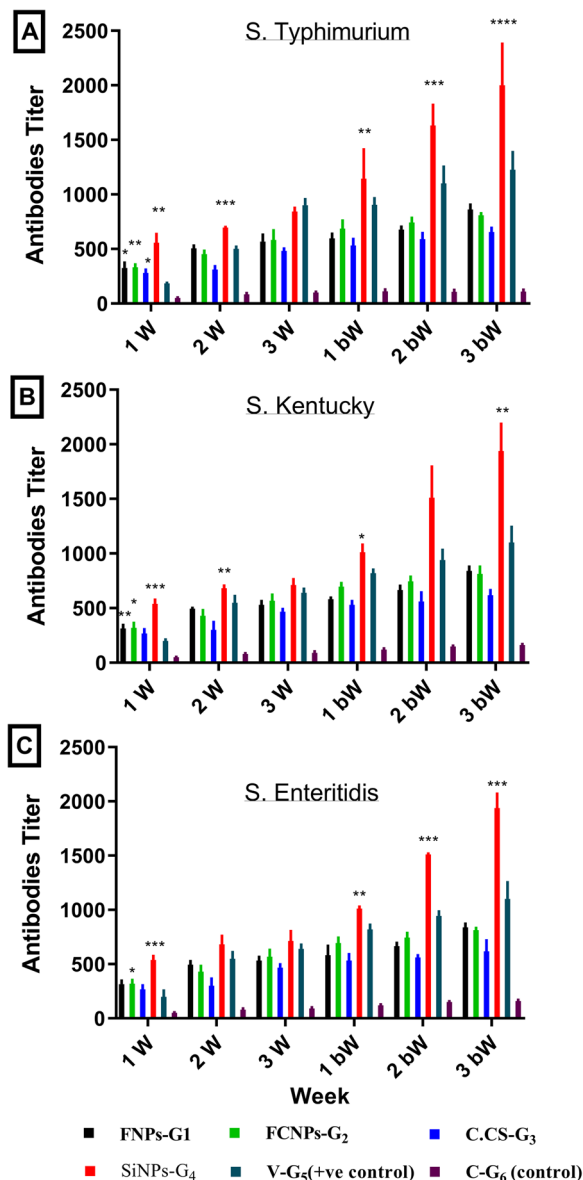


**Fig. 5** Antibody titer against **A** *S. Typhimurium*, **B** *S. Kentucky*, and **C** *S. Enteritidis* in sera of chicken vaccinated with trivalent *Salmonella* nanovaccines as measured by ELISA, bW represents post-booster week. Significant at  $p < 0.05$ ,  $**p < 0.01$ ,  $***p < 0.001$ , and  $****p < 0.0001$

titer increase from 415 (first week post-vaccination) to 937 after booster immunization. A similar pattern was observed in other groups, emphasizing the varied antibody responses. Statistical analysis reaffirmed the SiNPs-G4 group’s heightened antibody titer compared to other groups, underscoring its immunogenic potential.

The statistical analysis using one-way ANOVA Dunnett’s multiple comparisons test yielded the following results (Fig. 6): When compared to the control group (C-G6), FNPs-G1 and FCNPs-G2 supplementation had a significant impact on the measured parameter. In contrast, C.CS-G3 supplementation did not show a significant difference compared to the control group. On the other hand, SiNPs-G4 supplementation resulted in a significant impact in the measured parameter, while V-G5 (+ve control) supplementation also exhibited a significant impact. In summary, all supplementation regimens, except for C.CS-G3, were significantly influenced. Among the evaluated regimens, SiNPs-G4 showed the highest impact, followed by V-G5, while FNPs-G1 and FCNPs-G2 had similar effects. Therefore, based on these findings, the ranking of the trivalent nanovaccines in terms of their effectiveness for the measured parameter

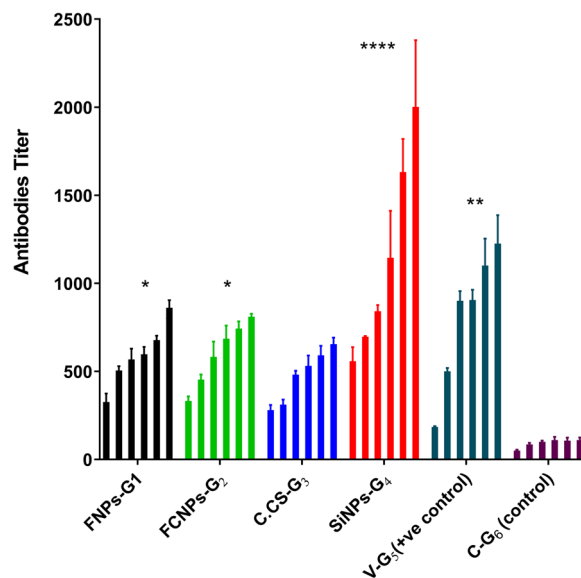


**Fig. 6** Dunnett’s multiple comparisons test— one-way ANOVA results for the comparison between the control group (C-G6) and various nanovaccines groups: FNPs-G1, FCNPs-G2, C.CS-G3, SiNPs-G4, and V-G5 (+ve control). Significant impacts were observed in SiNPs-G4 (\*\*\*), V-G5 (\*\*), FNPs-G1 and FCNPs-G2 (\*), while no significant difference was found for C.CS-G3 (ns), bW represents post-booster week.  $*p < 0.05$ ,  $**p < 0.01$ ,  $***p < 0.001$ , and  $****p < 0.0001$

is as follows: SiNPs-G4 > V-G5 > FNPs-G1 = FCNPs-G2. This suggests that SiNPs-G4 is the most effective trivalent nanovaccine, followed by V-G5, while FNPs-G1 and FCNPs-G2 exhibit comparable effectiveness. These results highlight the potential of SiNPs-G4 and V-G5 as promising options for further exploration and development in the field of trivalent nanovaccines.

## 4.2 Challenge test

### 4.2.1 Protection rate

The protection rate was evaluated by challenge test which done on vaccinated chicken as shown in Table 2 explains that the protection rate in the first group was 92% while the mortality rate was 10%; in the second group the protection rate was 67%, while the mortality rate was 33%; in the third group, the protection rate was 83%, mortality rate was 17%, and in the fourth group the protection rate was 93% and mortality rate was 7%.

Silicon dioxide nanoparticles have the highest protection rate among groups. In the fifth group, the protection rate was 86% while a mortality rate was 14%, while in the negative control group, the protection rate was 11% while the mortality rate was 89%. From Table 2, silicon dioxide and iron oxide nanoparticles enhanced the protection against trivalent *Salmonella* strains more than locally obtained vaccine.

### 4.2.2 Fecal shedding

The vaccinated chicken have fecal shedding of *Salmonella* organisms in Table 3, which was 12% in the first week and decline to 7% in the first group, in the second group was 50% and decreased to 16.6%, in the third group fecal shedding was 46% till reached 10.6%, in the fourth group was 17.8% and decreased to 6%, in the fifth group was 12.6% and decreased to 6.89% and in the unvaccinated control group, fecal shedding was observed in 50% of the individuals at 3 weeks post-challenge, which increased to 70%. In the vaccinated group, no shedding was detected at the fourth week post-challenge, while the control unvaccinated group had a 20% shedding rate.

## 4.3 Discussion

The experimental data acquired from zeta potential measurements, hydrodynamic diameter distribution, TEM analysis, and XRD patterns provide valuable insights into the stability, size, uniformity, morphology, and crystalline nature of the synthesized nanoparticles. Zeta potential analysis (Fig. 1a) revealed the stability of Fe<sub>2</sub>O<sub>3</sub>, Fe<sub>2</sub>O<sub>3</sub>-CS, C.CS, and SiO<sub>2</sub> nanoparticles, with potentials of 32.2 ± 5.01, 38.8 ± 6.06, 45.2 ± 5.02, and -45.8 ± 6.14 mV, respectively. All these values exceeded the stability range of ± 30 mV [28, 35–37]. Additionally, hydrodynamic diameter distributions (Fig. 1b) indicated

sizes of 81.95 ± 14.95 nm (Fe<sub>2</sub>O<sub>3</sub>), 137.1 ± 20.5 nm (Fe<sub>2</sub>O<sub>3</sub>-CS), 32.86 ± 14.05 nm (C.CS), and 15.64 ± 3.6 nm (SiO<sub>2</sub>) using dynamic light scattering.

The TEM images (Fig. 2A–D) displayed well-defined structures and sizes of the nanomaterials, confirming the crystalline nature. The XRD patterns (Fig. 3) matched standard hematite and confirmed the successful synthesis of Fe<sub>2</sub>O<sub>3</sub> and Fe<sub>2</sub>O<sub>3</sub>-CS nanomaterials. The XRD of SiO<sub>2</sub> indicated its amorphous nature, while C.CS exhibited a semi-crystalline structure. The Fe<sub>2</sub>O<sub>3</sub>-CS NPs showed a shift and reduction in the chitosan peak, indicating successful binding to Fe<sub>2</sub>O<sub>3</sub> NPs without inducing phase changes.

The MIC results indicated that FNPs, FCS NPs, C.CS NPs, and SiNPs exhibit antibacterial properties against three *Salmonella* strains. MIC values obtained for FNPs and FCS NPs are consistent with a previous study [38] that investigated the MIC of sonicated FNPs against gram-negative bacteria strains. Similarly, the MIC of C.CS NPs aligns with the findings of [39], which reported that chitosan does not have a bactericidal or bacteriostatic effect against *S. Typhimurium*. Confocal live/dead imaging results revealed that at a concentration of 200 µg/mL, none of the nanomaterials significantly affected bacterial viability. However, at 400 µg/mL, all nanomaterials, except SiNPs, exhibited a notable reduction in bacterial viability. This suggests that higher concentrations of nanomaterials can enhance the antibacterial activity. It is important to note that we focused on the antibacterial effects of the tested nanomaterials on *Salmonella* strains. Further research is needed to evaluate their effects on other bacterial species and assess their biocompatibility and potential cytotoxicity. Additionally, investigating the underlying mechanisms of action of these nanomaterials against bacteria would provide a deeper understanding of their antimicrobial properties.

Choosing the right adjuvant to elicit a robust humoral and cellular immune response in animals is a complex process. This choice hinges on considerations of safety, biodegradability, stability, cost-effectiveness, and immunogenic potency. Nanomaterials present a compelling solution, offering these properties, but the specific nanomaterials used as adjuvants play a pivotal role in this equation. In our vaccination and challenge tests against tri-*Salmonella* strains, it became evident that nanovaccines, particularly those employing silicon dioxide nanoparticles (SiNPs), have the capacity to enhance humoral immune response. These nanomaterials are smaller in diameter (15.64 ± 3.6 nm) compared to bacterial pores, possess the unique capability to penetrate the cell membrane, disrupt its function, interfere with nucleic acid or protein synthesis, and exhibit large molecular diffusion and adsorption capacity. This has been supported

**Table 2** The protection and mortality rate among vaccinated chicken

Groups	No. of birds	No. of diseased/Weeks post-challenge				Diseased/Total	No. of Survival	Total no. of survival	Mortality rate	Protection rate
		1st week	2nd week	3rd week	4th week					
FNPs-G <sub>1</sub>	10 (ST)	1	0	0	0	1/10	9	26/30	13.3	86.67
	10 (SK)	2	0	0	0	2/10	8			
FCNPs-G <sub>2</sub>	10 (SE)	1	0	0	0	1/10	9			
	10 (ST)	2	0	1	0	3/10	7	20/30	33	67
	10 (SK)	1	1	1	0	3/10	7			
	10 (SE)	2	1	1	0	4/10	6			
C-CS-G <sub>3</sub>	10 (ST)	1	1	0	0	2/10	8	24/30	20	80
	10 (SK)	1	1	0	0	2/10	8			
	10 (SE)	1	0	1	0	2/10	8			
	10 (ST)	1	0	0	0	0/10	10	28/30	6.67	93.33
SiNPs-G <sub>4</sub> *	10 (SK)	1	0	0	0	1/10	9			
	10 (SE)	1	0	0	0	1/10	9			
	10 (ST)	1	0	1	0	2/10	8			
	10 (SK)	1	0	0	0	0/10	10	28/30	6.67	93.33
V-G <sub>5</sub> (+ve Control)	10 (ST)	1	0	1	0	2/10	8	25/30	16.67	83.33
	10 (SK)	1	1	0	0	2/10	8			
	10 (SE)	1	0	0	0	1/10	9			
	10 (ST)	4	3	1	1	9/10	1	9/10	90	10
C-G <sub>6</sub> (control)	10 (SK)	3	3	2	1	9/10	1	9/10	90	10
	10 (SE)	5	3	1	0	9/10	1	9/10	90	10
	10 (ST)	1	0	0	0	1/10	9			

\*p<0.05, \*\*p<0.01, \*\*\*p<0.001, and \*\*\*\*p<0.0001

**Table 3** Re-isolation of *Salmonella* after challenge test

Groups	No. of birds positive for isolation/total No. of living birds*100%			
	1st week %	2nd week %	3rd week %	4th week %
FNPs-G <sub>1</sub> *	12	9.6	7	0
FCNPs-G <sub>2</sub> *	50	30	16.6	0
C.CS-G <sub>3</sub>	46	12	10.6	0
SiNPs-G <sub>4</sub> ***	10.3	9	6	0
V-G <sub>5</sub> (+ve control)**	12.6	10.3	6.89	0
C-G <sub>6</sub> (control)	50	80	70	20

\* $p < 0.05$ , \*\* $p < 0.01$ , \*\*\* $p < 0.001$ , and \*\*\*\* $p < 0.0001$

by studies [40, 41]. SiNPs, notably, yielded a more robust immune response compared to chitosan nanoparticles, widely used in various studies. For instance, a study by [42] who used chitosan-*Salmonella* subunit nanovaccines for chicken giving a good immune response to the vaccinated chicken, [40] proved that SiNPs work as a good adjuvant in vaccines as it has good stability and non-lytic for more than six months.

While ferric oxide with diameter size ( $81.95 \pm 14.95$  nm) gives a good immune response, it is less effective than silicon dioxide as shown in previous studies using ferric oxide nanoparticles with different diameter sizes. For example, Ban et al. demonstrated that in mice with mean diameters of  $35 \pm 14$  nm and  $147 \pm 48$  nm, respectively, allergic T-helper cell responses induced by Ovalbumin antigen were suppressed [22]. Not only the diameter size but the surface charge is a necessary parameter for vaccine design strategies due to its important role in the recruitment of antigen-presenting cells [23]. When compared to anionic-charged NPs, cationic-charged NPs improved the cross-presentation of delivery cells. The relationship between increased cytosolic antigen delivery and increased cross-presentation given by cationic-charged NPs shows that positively charged NPs' ability to transfer antigens into the cytoplasm is beneficial for both T cell activation and cross-presentation of antigens. So, surface coatings and the shape of ferric oxide are two of the main characteristics playing an important role in adjuvanticity.

Using ferric oxide with chitosan gives low titer of antibodies against *Salmonella* strains and these findings in contrast to [11] who used carboxymethyl chitosan bounded iron oxide nanoparticles were effective on enhancing immunogenicity as irradiated Avian influenza virus antigen administered with a clinically acceptable adjuvant. Using carboxy methyl chitosan as it has the properties of high aqueous solubility, high charge density, mucoadhesive, permeation enhancing (ability to

cross tight junction), and stability over a range of ionic conditions, which makes the spectrum of its applicability much broader, and there is lesser work on it, so we use it but it gives low antibodies titer against *Salmonella* strains and these findings was in contrast to [43] who used trimethyl chitosan nanoparticles as an adjuvant. Prepared nanovaccines gives higher immune response against *Salmonella* strains than locally prepared inactivated *Salmonella* vaccine adjuvanted with formalin, which have high toxicity and carcinogenicity. Based on the data presented in Fig. 5, it can be concluded that all five vaccine formulations induced an immune response against *Salmonella* in vaccinated chicken, as demonstrated by the increase in antibody titers over time. However, the magnitude of the immune response varied among the different vaccine formulations. The highest antibody titer was observed in the SiNPs-G4 group, followed by the V-G5 group. These findings suggest that the use of silicon dioxide nanoparticles as a vaccine delivery system may enhance the immune response to *Salmonella* in chicken.

Silicon dioxide nanoparticles have the highest protection rate among groups. due to its unique properties, such as good chemical properties, small particles size, and good stability, which results in large specific surface-area to volume ratio, strong adsorption capacity, and insulation, these findings were in parallel with [18] who used it as vaccine carrier and give good protection rate, and these findings were agreed with [11]. Furthermore, the trivalent nanovaccines demonstrated a high protection rate against *Salmonella* strains, with SiNPs-G4. Fecal shedding was significantly reduced in the vaccinated groups compared to the control group. Fecal shedding findings of *Salmonella* were in accordance with [21]. These results highlight the potential of trivalent nanovaccines, particularly those utilizing silicon dioxide nanoparticles, as effective strategies for enhancing immune response and protection against *Salmonella* in poultry.

#### 4.4 Conclusion

This study explored nanomaterials to boost the immune response against *Salmonella* in chickens. Incorporating iron oxide (FNPs), silicon dioxide (SiNPs), carboxymethyl chitosan (C.CS NPs), and iron oxide with chitosan (FCNPs) nanomaterials in the vaccine improved its efficacy, evident from significant differences within and between groups. This suggests nanomaterials inclusion as a promising strategy to control chicken salmonellosis. All four vaccine formulations induced an immune response against *S. Enteritidis* in chickens, as seen in the increasing antibody titers over time. The SiNPs-G4 group exhibited the highest antibody titer, implying the potential of silicon nanoparticles in enhancing the immune response.

Further research is needed to explore these nanomaterials in different animal models and assess their safety and long-term effects.

#### Abbreviations

AO	Acridine orange
C.CS	Carboxymethyl chitosan
C.CS NPs	Carboxymethyl chitosan nanoparticles
CFU/mL	Colony-forming units per milliliter
Fe <sub>2</sub> O <sub>3</sub>	Ferrous iron oxide
FCNPs	FNPs-chitosan nanoparticles
FNPs	Fe <sub>2</sub> O <sub>3</sub> nanoparticles
LB	Luria broth
MIC	The minimum inhibitory concentration
NH <sub>4</sub> OH	Ammonium hydroxide
NPs	Nanoparticles
PI	Propidium iodide
PVP	Polyvinylpyrrolidone
S.	Salmonella
SiO <sub>2</sub>	Silicon dioxide
SiNPs	Silicon dioxide nanoparticles
SPF	Specific pathogen-free
TEM	Transmission electron microscopy
TEOS	Tetraethylorthosilicate
TPP	Sodium tripolyphosphate
ZPs	Zeta potentials

#### Acknowledgements

Not applicable.

#### Author contributions

HMI, GMM, RHS did conceptualization, methodology, data acquisition, validation, formal analysis, resources, and review & editing. HAE done conceptualization, methodology, data acquisition, validation, formal analysis, supervision, resources & funding, and review & editing. HEE and ShAE performed methodology, data acquisition, validation, and revising the original draft. All authors read and approved the final manuscript.

#### Funding

This work was financially supported by the Joint Research Project between The Institute of Biophysics and Biomedical Engineering, Bulgarian Academy of Sciences, Bulgaria, and The Academy of Scientific Research and Technology (ASRT), Egypt, and Nanotechnology and Advanced Materials Central Lab, Agricultural Research Centre, Egypt entitled "Biological activity of Nanocomposites materials with potential medical and microbiology application".

#### Availability of data and materials

Data are available upon request.

#### Declarations

##### Ethics approval and consent to participate

Institutional Animal Care and Use Committee at Central Laboratory for Evaluation of Veterinary Biologics hereby acknowledges that the research manuscript has been reviewed under our research authority and is deemed in compliance with bioethical standards in good faith.

##### Consent for publication

Not applicable.

##### Competing interests

The authors declare that they have no competing interests.

#### References

- Renu S, Markazi AD, Dhakal S, Lakshmanappa YS, Shanmugasundaram R, Selvaraj RK, Renukaradhya GJ (2020) Oral deliverable mucoadhesive chitosan-Salmonella subunit nanovaccine for layer chickens. *Int J Nanomedicine* 15:761–777
- Majowicz SE, Musto J, Scallan E, Angulo FJ, Kirk M, O'Brien SJ, Jones TF, Fazil A, Hoekstra RM (2010) The global burden of nontyphoidal Salmonella gastroenteritis. *Clin Infect Dis* 50:882–889. <https://doi.org/10.1086/650733>
- Cogan TA, Humphrey TJ (2003) The rise and fall of Salmonella Enteritidis in the UK. *J Appl Microbiol* 94:114–119. <https://doi.org/10.1046/j.1365-2672.94.s1.13.x>
- Varmuzova K, Faldynova M, Elsheimer-Matulova M, Sebkova A, Polansky O, Havlickova H, Sisak F, Rychlik I (2016) Immune protection of chickens conferred by a vaccine consisting of attenuated strains of Salmonella Enteritidis, Typhimurium and Infantis. *Vet Res* 47:94. <https://doi.org/10.1186/s13567-016-0371-8>
- Rabie NS, Ibrahim HM, Ghetas AM, Abdelbaki MM, Fedawy HS, Sedeek DM, Bosila MA, Elbayoumi KM, Samy AA (2023) Trial for preparation and evaluation of autogenous killed vaccine against some locally isolated strains of *Salmonella enterica* from chickens in Egypt. *Int J Vet Sci* 12:456–461. <https://doi.org/10.47278/journal.ijvs/2022.209>
- Ibrahim H, Sayed R, Am S (2018) Efficacy of a locally prepared inactivated trivalent vaccine against Salmonellosis in poultry. *Int J Vet Sci* 7:82–87
- Paudel S, Hess C, Kamal Abdelhamid M, Lyrakis M, Wijewardana V, Thiga Kangethe R, Cattoli G, Hess M (2023) Aerosol delivered irradiated *Escherichia coli* confers serotype-independent protection and prevents colibacillosis in young chickens. *Vaccine* 41:1342–1353. <https://doi.org/10.1016/j.vaccine.2022.12.002>
- Zhou X, Richards P, Windhorst D, Imre A, Bukovinski A, Ruggeri J, Elazomi A, Barrow P (2022) Generation of an inactivated vaccine for avian pathogenic *Escherichia coli* using microarrays: a more rational approach to inactivated vaccine design. *Open Vet J* 12:221–230. <https://doi.org/10.5455/OVJ.2022.v12.i2.10>
- Rabie NS, Amin Girh ZMS (2020) Bacterial vaccines in poultry. *Bull Natl Res Cent* 44:1–7. <https://doi.org/10.1186/s42269-019-0260-1>
- Nahla MS, Slim SA, Yassin BR (2014) Preparation and evaluation of avian pathogenic *E. coli* lipopolysaccharide and ribosomal vaccines against avian colibacillosis in broiler chicken in Al-Sulaimania Province, Assiut. *Vet Med J* 61:24–31. <https://doi.org/10.1608/avmj.2014.169745>
- Motamedi-sedeh F, Saboorizadeh A, Khalili I, Sharbatdaran M, Wijewardana V, Arbabi A (2022) Carboxymethyl chitosan bounded iron oxide nanoparticles and gamma-irradiated avian influenza subtype H9N2 vaccine to development of immunity on mouse and chicken. *Vet Med Sci* 8:626–634. <https://doi.org/10.1002/vms3.680>
- Alshehri MM, Sharifi-rad J, Herrera-bravo J, Jara EL, Salazar LA, Kregiel D, Uprety Y, Akram M, Iqbal M, Martorell M, Torrens-mas M (2021) Review article therapeutic potential of isoflavones with an emphasis on daidzein. *Oxid Med Cell Longev* 2021:1–15
- Khan S, Khan A, Rehman AU, Ahmad I, Ullah S, Khan AA, Ali SS, Afridi SG, Wei D-Q (2019) Immunoinformatics and structural vaccinology driven prediction of multi-epitope vaccine against Mayaro virus and validation through in-silico expression. *Infect Genet Evol* 73:390–400. <https://doi.org/10.1016/j.meegid.2019.06.006>
- Pogostin BH, Mchugh KJ (2021) Novel vaccine adjuvants as key tools for improving pandemic preparedness. *Bioengineering* 8:1–16
- Saleem AF, Yousafzai MT, Mach O, Khan A, Quadri F, Weldon WC, Oberste MS, Zaidi SS, Alam MM, Sutter RW, Zaidi AKM (2018) Evaluation of vaccine derived poliovirus type 2 outbreak response options: a randomized controlled trial, Karachi, Pakistan. *Vaccine* 36:1766–1771. <https://doi.org/10.1016/j.vaccine.2018.02.051>
- Mitchell MJ, Billingsley MM, Haley RM, Wechsler ME, Peppas NA, Langer R (2021) Engineering precision nanoparticles for drug delivery. *Nat Rev Drug Discov* 20:101–124. <https://doi.org/10.1038/s41573-020-0090-8>
- Iacob M, Racles C, Dascalu M, Tugui C, Lozan V, Cazacu M (2019) Nanomaterials developed by processing iron coordination compounds for biomedical application. *J Nanomater* 2019:2592974. <https://doi.org/10.1155/2019/2592974>

Received: 6 June 2023 Accepted: 18 February 2024

Published online: 29 February 2024

18. Skrastina D, Petrovskis I, Lieknina I, Bogans J, Renhofa R, Ose V, Dishlers A, Dekhtyar Y, Pumpens P (2014) Silica nanoparticles as the adjuvant for the immunisation of mice using hepatitis B core virus-like particles. *PLoS ONE* 9:4006. <https://doi.org/10.1371/journal.pone.0114006>
19. Virginio VG, Bandeira NC, Munhoz F, Lancellotti M, Zaha A, Ferreira HB (2017) Assessment of the adjuvant activity of mesoporous silica nanoparticles in recombinant *Mycoplasma hyopneumoniae* antigen vaccines. *Heliyon*. <https://doi.org/10.1016/j.heliyon.2016.e00225>
20. Virginio VG, Bandeira NC, Leal FMA, Lancellotti M, Zaha A, Ferreira HB (2017) Assessment of the adjuvant activity of mesoporous silica nanoparticles in recombinant *Mycoplasma hyopneumoniae* antigen vaccines. *Heliyon* 3:e00225. <https://doi.org/10.1016/j.heliyon.2016.e00225>
21. Ibrahim HM, Sayed R, Shereen A (2018) Efficacy of a locally prepared inactivated trivalent vaccine against salmonellosis in poultry. *Int J Vet Sci* 7:82–87
22. Ban M, Langonné I, Huguet N, Guichard Y, Goutet M (2013) Iron oxide particles modulate the ovalbumin-induced Th2 immune response in mice. *Toxicol Lett* 216:31–39. <https://doi.org/10.1016/J.TOXLET.2012.11.003>
23. Mou Y, Xing Y, Ren H, Cui Z, Zhang Y, Yu G, Urba WJ, Hu Q, Hu H (2017) The effect of superparamagnetic iron oxide nanoparticle surface charge on antigen cross-presentation. *Nanoscale Res Lett*. <https://doi.org/10.1186/s11671-017-1828-z>
24. Motamedi-sedeh F, Sharbatdaran M, Saboorzadeh A, Wijewardana V, Khalili I, Arbabi A (2022) Carboxymethyl chitosan bounded iron oxide nanoparticles and gamma-irradiated avian influenza subtype H9N2 vaccine to development of immunity on mouse and chicken. *Vet Med Sci* 8:626–634. <https://doi.org/10.1002/vms3.680>
25. Charles SD, Hussain I, Choi CU, Nagaraja KV, Sivanandan V (1994) Adjuvanted subunit vaccines for the control of *Salmonella enteritidis* infection in turkeys. *Am J Vet Res* 55:636–642
26. Krug HF (2011) Hydrothermal synthesis of UC-Fe<sub>3</sub>O<sub>4</sub>\_50-1\_v4 - Hydrothermal synthesis of PVP capped Fe<sub>3</sub>O<sub>4</sub> nanoparticles, in: *Compr. Assess. Hazard. Eff. Eng. Nanomater. Immune Syst. Qual. Handb. Stand. Proced. Nanoparticle Test.*, pp 63–86
27. Sun X, Zhang J, Chen Y, Mi Y, Tan W, Li Q, Dong F, Guo Z (2019) Synthesis, characterization, and the antioxidant activity of carboxymethyl chitosan derivatives containing thiourea salts. *Polym Artic* 11:1–16
28. El-sayed NM, El-bakary MA, Ibrahim MA, Elgamal MA, Elsayed H, Elshoky HA (2023) Synthesis and characterization of mussel-inspired nanocomposites based on dopamine–chitosan–iron oxide for wound healing: in vitro study. *Int J Pharm* 632:122538. <https://doi.org/10.1016/j.ijpharm.2022.122538>
29. ElZorkany HE, Farroh KY, El-Shorbagy HM, Elshoky HA, Youssef T, Salaheldin TA, Sabet S (2022) Silica-coated graphene compared to Si-CdSe/ZnS quantum dots: toxicity, emission stability, and role of silica in the uptake process for imaging purposes. *Photodiagnosis Photodyn Ther* 39:102919. <https://doi.org/10.1016/j.pdpdt.2022.102919>
30. Jiao L, Lin F, Cao S, Wang C, Wu H, Shu M, Hu C (2017) Preparation, characterization, antimicrobial and cytotoxicity studies of copper/zinc-loaded montmorillonite. *J Anim Sci Biotechnol* 8:1–7. <https://doi.org/10.1186/s40104-017-0156-6>
31. OIE Terrestrial Manual (2018) Tests For Sterility and Freedom from Contamination of Biological Materials Intended For Veterinary Use, in: *OIE Terr. Man.*, 2018, pp 109–122
32. Mousa HA (2007) Bones and joints tuberculosis, Bahrain. *Med Bull* 29:1–9
33. Cruickshank JJ, Sim JS (1987) Effects of excess vitamin D<sub>3</sub> and cage density on the incidence of leg abnormalities in broiler chickens. *Avian Dis* 31:332–338. <https://doi.org/10.2307/1590881>
34. Snedecor GW, Cochran WG (1980) *Statistical methods*, 7th ed
35. Elshoky HA, El-Sayed NM, Hassouna YH, Salaheldin TA, Gaber MH, Ali MA (2023) Improved in vitro biocompatibility and cytoplasmic localization of gold nanoparticles and graphene oxide nanosheets assessed using confocal microscopy. *J Drug Deliv Sci Technol*. <https://doi.org/10.1016/j.jddst.2023.104678>
36. Milad SS, Ali SE, Attia MZ, Khattab MS, El-Ashaal ES, Elshoky HA, Azouz AM (2023) Enhanced immune responses in dexamethasone immunosuppressed male rats supplemented with herbal extracts, chitosan nanoparticles, and their conjugates. *Int J Biol Macromol* 250:1261. <https://doi.org/10.1016/j.jbiomac.2023.126170>
37. Abd El-Aziz WR, Ibrahim HM, Elzorkany HE, Mohammed GM, Mikhael CA, Fathy NA, Elshoky HA (2022) Evaluation of cell-mediated immunity of *E. coli* nanovaccines in chickens. *J Immunol Methods* 506:1–9. <https://doi.org/10.1016/j.jim.2022.113280>
38. Al-Rawi M, Al-Mudallal NHAL, Taha AA (2021) Determination of ferrous oxide nanoparticles minimum inhibitory concentration against local virulent bacterial isolates. *Arch Razi Inst* 76:796. <https://doi.org/10.22092/ari.2021.355997.1758>
39. Ibañez-Peinado D, Ubeda-Manzanaro M, Martínez A, Rodrigo D (2020) Antimicrobial effect of insect chitosan on *Salmonella Typhimurium*, *Escherichia coli* O157:H7 and *Listeria monocytogenes* survival. *PLoS ONE*. <https://doi.org/10.1371/journal.pone.0244153>
40. Huang X, Townley HE (2020) An assessment of mesoporous silica nanoparticle architectures as antigen carriers. *Pharmaceutics*. <https://doi.org/10.3390/pharmaceutics12030294>
41. Mody KT, Popat A, Mahony D, Cavallaro AS, Yu C, Mitter N (2013) Mesoporous silica nanoparticles as antigen carriers and adjuvants for vaccine delivery. *Nanoscale* 5:5167–5179. <https://doi.org/10.1039/c3nr00357d>
42. Renu S, Han Y, Dhakal S, Lakshmanappa YS, Ghimire S, Feliciano-Ruiz N, Senapati S, Narasimhan B, Selvaraj R, Renukaradhya GJ (2020) Chitosan-adjuvanted *Salmonella* subunit nanoparticle vaccine for poultry delivered through drinking water and feed. *Carbohydr Polym* 243:116434. <https://doi.org/10.1016/j.carbpol.2020.116434>
43. Malik A, Gupta M, Gupta V, Gogoi H, Bhatnagar R (2018) Novel application of trimethyl chitosan as an adjuvant in vaccine delivery. *Int J Nanomed* 13:7959–7970. <https://doi.org/10.2147/IJN.S165876>

## Publisher's Note

Springer Nature remains neutral with regard to jurisdictional claims in published maps and institutional affiliations.